Individual Off-axis Refraction Patterns in Orthokeratology for Different Myopic Treatments

[1]QUEIRÓS A., [1]GONZÁLEZ-MÉIJOME J.M., [1]JORGE J., [2]VILLA-COLLAR C., [3]GUTIÉRREZ J.R.

[1]School of Science (Optometry), University of Minho, Braga, Portugal; [2]Clínica Oftalmológica Novovision, Madrid, Spain;
[3]Department of Ophthalmology, University of Murcia, Murcia, Spain

INTRODUCTION

Myopia affects approximately 25% of the World population and has become a public health concern due to the socioeconomic impact and to the risk of vision loss related to other co-morbidities.[1] For these reasons there is great interest in solutions to prevent myopia onset and progression. Given the lack of effect on axial elongation of conventional geometry lenses,[2] the most promising approach involving contact lenses for slowing myopia progression consists of myopia correction with reverse geometry contact lenses for corneal reshaping.

The hypothesized reason for corneal reshaping interfering with the ocular growth pattern is that it induces a myopic change in relative peripheral refractive error (RPRE) while the central refraction is fully corrected. According to this theory, the myopic RPRE following CRT prevents the hyperopic RPRE usually present in the myopic eye from acting as a stimulus for ocular growth, as has been suggested in animal models.[3-7]

The purpose of this study was to characterize the central and peripheral refraction across the horizontal meridian of the visual field before and after corneal refractive therapy (CRT) with contact lenses for different degrees of myopic correction.

MATERIAL AND METHODS

Subjects and inclusion criteria

Measurements were made on twenty-eight right eyes of 34 university students with a mean age of 25.2±6.4 years (ranging from 20 to 41), of which 11 were female (39.3%) and 17 were male (60.7%). Total preoperative spherical equivalent obtained with subjective refraction was -2.15±1.26D (from -0.88 to -5.25D). Subjective non-cycloplegic refraction was performed monocularly.

Peripheral Refraction

The measurement of central and peripheral refraction was obtained with the open-field Grand Seiko Auto-Refractometer/Keratometer WAM-5500 (Grand Seiko Co., Ltd., Hiroshima, Japan). The illumination of the room was adjusted to obtain a pupil size greater than 4mm required to allow peripheral measurements, which was achieved in all cases. The fixation target was placed at a distance of 2.5 meters from the patient's corneal vertex and consisted of 15 LEDs in the horizontal direction: one central, seven to the right and seven to the left side. The LEDs were separated from each other by an angular distance of 5° at the patient's position. Five readings were taken and averaged only on the right eye of each individual in all positions. The axis of the autorefractor was aligned with the center of the entrance pupil during all measurements.

Analysis was stratified into four different myopic ranges according to the spherical baseline refraction as Group 1 [-0.50 to -1.00D; n=9], Group 2 [-1.25 to -1.75D; n=11], Group 3 [-2.00 to -2.75D; n=8] and Group 4 [-3.00 to -5.50D; n=6].

Descriptive statistics (mean±S.D.) were obtained for the refraction vector components.

Corneal refractive therapy lens characteristics

Paragon CRT™ (paflufocon D, Dk=100 barrer) sigmoid reverse geometry rigid gas permeable lenses were used (Paragon Vision Sciences, Mesa, AZ, USA). Parameters of the CRT™ lenses were (mean±S.D. [minimum, maximum]), base curve radius: (BCR=8.38±0.29mm [7.90,9.00 mm]), return zone depth: (RZD=530.88± 18.52µm [500,575 µm]) and landing zone angle: (LZA=32.85±0.66 degrees [31.00,34.00 degrees]). A minimum treatment period of one month was required to guarantee that the treatment was completely stable.[8] The time between pre and post treatment measures was 37.0±3.0 days. During that period, lenses were worn overnight for 7.82±1.02 hours.

RESULTS

Statistically significant differences were found for the spherical equivalent (diff post-pre= +1.57±0.77D, p<0.001), but not for the astigmatic components J0 (p=0.778) and J45 (p=0.422).

In *figure 1*, spherical equivalent refraction shows a significant myopic reduction within the central 40°, being maximum at the center. At 25° however, the treatment showed no effect on the M component, while a myopic increase is noticed beyond the central 50° of the visual field (25° along to each side). For astigmatism components, again no significant differences exist for the J0 component within the central 20° (10° to each side), but a significant increase in myopic astigmatism is observed beyond this point. Conversely, no consistent significant changes were noticed across the field for the J45 component.

Figure 2 shows the degree of peripheral myopia induced by CRT (average values from nasal and temporal locations) as a function of individual baseline M component. This analysis showed that peripheral values obtained at 30° (r^2=0.573, p<0.001) and 35° (r^2=0.645, p<0.001) reflect the higher correlation with baseline spherical equivalent refraction. For those locations, there was a linear regression line that describes a nearly 1:1 relationship between average change in spherical equivalent for a given peripheral eccentric refraction (homologous nasal and temporal locations) and the axial spherical equivalent at baseline.

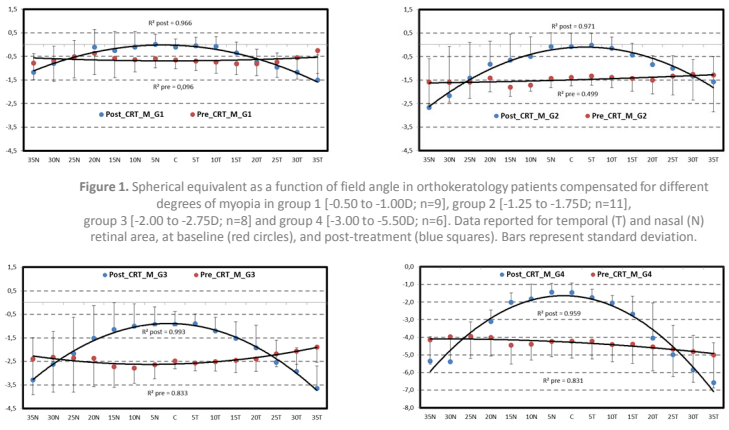

Figure 1. Spherical equivalent as a function of field angle in orthokeratology patients compensated for different degrees of myopia in group 1 [-0.50 to -1.00D; n=9], group 2 [-1.25 to -1.75D; n=11], group 3 [-2.00 to -2.75D; n=8] and group 4 [-3.00 to -5.50D; n=6]. Data reported for temporal (T) and nasal (N) retinal area, at baseline (red circles), and post-treatment (blue squares). Bars represent standard deviation.

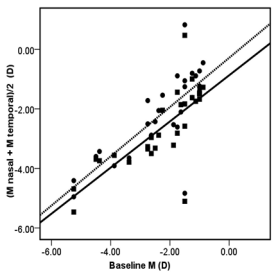

▲ **Figure 2.**
Change in spherical equivalent after CRT for a given peripheral eccentric location [(M nasal + M temporal)/2] as a function of the axial spherical equivalent at baseline. For clarity, only the higher correlations are shown, corresponding to the 30° (r^2=0.573, circles, point line,) and 35° (r^2=0.645, squares, full line) eccentric locations.

CONCLUSIONS

- Therapy corneal refractive reverses the pattern of refraction peripheral, both in its component areas such as spherical equivalent, creating an area reduction of myopia within 50° central visual field and increase it beyond 50 degrees.
- We found that changes in astigmatism were statistically significant only in the J0 component, from the 15° or 20° in the nasal and temporal directions (30 ° to 40 ° central field amplitude).
- On the peripheral refraction of 30° and 35°, the degree of induced myopia in terms of spherical equivalent has a ratio of almost 1:1 with the reference quantity of refraction spherical equivalent to be corrected.
- **The inversion of the hyperopic trend in the peripheral field of vision of myopic eyes is only present when more than -2.50 D of myopia are corrected with orthokeratology. Below this level, the peripheral retina either remains hyperopic or emmetropic compared to axial refraction.**

REFERENCES

1. Kempen JH, Mitchell P, Lee KE et al. The prevalence of refractive errors among adults in the United States, Western Europe, and Australia. Arch.Ophthalmol 2004;122(4):495-505.
2. Walline JJ, Jones LA, Mutti DO, Zadnik K. A randomized trial of the effects of rigid contact lenses on myopia progression. Arch.Ophthalmol. 2004;122(12):1760-1766.
3. Smith EL, III, Kee CS, Ramamirtham R, Qiao-Grider Y, Hung LF. Peripheral vision can influence eye growth and refractive development in infant monkeys. Invest Ophthalmol Vis Sci 2005;46(11):3965-3972.
4. Smith EL, III, Ramamirtham R, Qiao-Grider Y et al. Effects of foveal ablation on emmetropization and form-deprivation myopia. Invest Ophthalmol Vis Sci 2007;48(9):3914-3922.
5. Diether S and Schaeffel F. Local changes in eye growth induced by imposed local refractive error despite active accommodation. Vision Res. 1997;37(6):659-668.
6. Charman WN, Mountford J, Atchison DA, Markwell EL. Peripheral refraction in orthokeratology patients. Optom Vis.Sci 2006;83(9):641-648.
7. Queirós, A., Gonzalez-Meijome, J. M., Jorge, J., Villa-Collar, C., and Gutierrez, A. R. (2010). Peripheral refraction in myopic patients after orthokeratology. Optom Vis Sci 87, 323-329.
8. Lu F, Simpson T, Sorbara L, Fonn D. The relationship between the treatment zone diameter and visual, optical and subjective performance in Corneal Refractive Therapy lens wearers. Ophthalmic Physiol Opt. 2007;27(6):568-578.

Acknowledgements

This work was supported by a grant from the Science and Technology Foundation (FCT) of Ministry of Science and Superior Education (MCES) (European Social Funding). Doctoral Fellowship (AQ) number SFRH/BD/61768/2009

FCT Fundação para a Ciência e a Tecnologia

Governo da República Portuguesa
União Europeia — Fundos Estruturais

Reprints: aqp@fisica.uminho.pt

The positive lenses for near work on the myopia shift in Chinese pre-myopic children – 6 month results

P.C. Wu

Dep. of Ophthalmology, Chang-Gung Memorial Hospital, Kaohsiung Medical Center, Taiwan.

INTRODUCTION

At present, the mechanisms involved in the etiology of myopia are unclear and means of prevention are unknown. Once elementary and junior high schoolchildren became myopia, then the myopia progression is irreversible (the rate is about -1D/year in Taiwan) and only atropine eye drop could slow down the progression. It results elongated eyeball axial length and finally it often develops high myopia, a predisposing factor for retinal detachment, myopic retinopathy, and glaucoma, thus contributing to loss of vision and blindness in both developed and developing countries.

The normal children refraction is mild hyperopia. The risk factors such as parents history, near work and lack of outdoor activity makes the hyperopia decrease and finally become myopia. In Taiwan, the prevalence of myopia increase rapidly recently, especially in kindergarten children (up to 20% in 6 y/o). How to maintain hyperopia and delay the myopia onset is an important issue.

Prolonged near work (e.g., reading) is associated with increased prevalence of myopia[9]. It develops the hypothesis that negating the prolonged chronic accommodation associated with near work would reduce myopia progression. The purpose of this study is to evaluate the effectiveness of near glasses with additional positive lenses (APLs), with a near addition of +1.50 D, for near work on the prevention of myopia shift and myopia onset in Chinese pre-myopic children.

METHODS

This study is a randomized, single-masked, controlled clinical trial. Children eligible for participation were 5-8 years of age with spherical refractive between +2.0 D and −0.50 D in both eyes, as measured by cycloplegic autorefraction; astigmatism ≤ 1.50 D; and no anisometropia, amblyopia and strabismus.

In the treatment group (APL group), children are prescribed near used glasses with additional positive lenses (spherical refraction +1.5D) in both eye and asked to wear this near glasses only when near work at least 1 hour everyday. In control group, there were no glasses prescribed. Both groups (children and parents) were educated to increase outdoor activities and reduce near work for preventing myopia onset.

The main study measures were cycloplegic autorefraction and axial length. Additional data of ocular examination and questionnaires were also collected. The data of right eye was conducted for analysis.

RESULTS:

Sixty-nine subjects (35 in control and 34 in APL) completed the 6-month study. There were no significant differences in age, sex and initial spherical equivalence between these 2 groups (Table 1).

The myopia shift (mean +/- S.D.) in the control groups and L group during 6M was -0.30 +/- 0.40 and -0.32 +/- 0.40 D, respectively. This difference of 0.02 D over 6M was not statistically significant (p = 0.82). Mean increase in the axial length was 0.25 +/- 0.38 and 0.23 +/- 0.34 mm, respectively. This difference of 0.02 mm was also not statistically significant (p = 0.85).

TABLE 1. Baseline demographic characteristics, initial and final spherical equivalent refraction, axial length and changes in different groups.

	Control group	APL group	*p*-value
N	35	34	
M/F	15/20	11/23	0.368
Age	6.6 ± 0.9	6.9 ± 0.8	0.140
Initial SER(D)	0.39 ± 0.57	0.36± 0.68	0.848
Initial AXL(mm)	22.7 ± 0.7	21.9 ± 3.5	0.209
Final SER(D)	0.06 ± 0.63	0.04 ± 0.83	0.886
Final AXL(mm)	22.9 ± 0.7	22.7 ± 0.8	0.328
Myopia shift (D/0.5 yr)	-0.30 ± 0.40	-0.32 ± 0.40	0.821
AXL increase (mm/0.5 yr)	0.23 ± 0.34	0.25 ± 0.37	0.801

M/F, male/female; SER, spherical equivalent refraction; D, diopter; yr, year;
* represents statistically significant (p<0.05)

In the multiple regression analysis, near papillary distance (NPD), father education (F edu), mother education (M edu), near work study time (Study time) had statistically significance associated with myopia shift (p=0.010, 0.039, 0.007 and 0.010, respectively, Table 2). Using the forward method of multiple regression analysis, only NPD and Study time had statistically significance. Smaller NPD and more study time would increase myopia shift.

Table 2. APL treatment and predictors of myopic shift using multiple linear regression analysis

	Myopic shift (D/yr)			
	unadjusted	adjusted	95% CI	p value
APL	0.09	0.15	(-0.12 ~ 0.31)	0.380
Gender	0.04	0.05	(-0.23 ~ 0.32)	0.753
Age	0.02	0.05	(-0.17 ~ 0.21)	0.821
ini SER	-0.11	-0.18	(-0.34 ~ 0.11)	0.301
NPD	0.10	0.61	(0.03 ~ 0.18)	0.010*
F edu	-0.20	-0.62	(-0.39 ~ -0.01)	0.039*
M edu	0.31	0.94	(0.09 ~ 0.53)	0.007*
F myo	-0.19	-0.33	(-0.49 ~ 0.10)	0.191
M myo	-0.01	-0.02	(-0.24 ~ 0.22)	0.937
Study time	-0.28	-0.60	(-0.48 ~ -0.08)	0.010*
Com game	0.03	0.09	(-0.12 ~ 0.18)	0.669
Near skill	-0.01	-0.02	(-0.13 ~ 0.11)	0.885
TV	-0.12	-0.26	(-0.31 ~ 0.08)	0.232
Outdoor	0.01	0.03	(-0.15 ~ 0.16)	0.903
Suppl. class	0.04	0.10	(-0.11 ~ 0.19)	0.585

NPD: near papillary distance; F edu: father education; M edu: mother education; F myopia: father myopia status; M myopia: mother myopia status; Study time: near work study time; Com game: computer or video games; near skill: skill for near work; TV: watching TV time; outdoor: outdoor activities; Suppl. Class: supplementary afterschool class.
*represent statistically significant, p<0.05

In the treatment group, there were 11 subjects (32%) with poor compliance. Poor compliance subjects had more myopia shift, however it was close but did not reaching statistical significance (p=0.088).

TABLE 3. Compare different compliance of APL treatment group during follow-up

	Poor compliance	Good compliance	p-value
N	11	23	
Myopia shift (D/0.5 yr)	-0.51 ± 0.30	-0.26 ± 0.40	0.088
AXL increase (mm/0.5 yr)	0.33 ± 0.45	0.18 ± 0.36	0.302

DISCUSSION

There was no significant benefit from near glasses with additional +1.5D positive lenses during near work in premyopic children. The possible reasons might be as following:

+1.5D lenses only partial relieve the strong and prolonged accommodation in near work.

+1.5D lenses is not enough to induce myopic defocus during near work.

Near work time, NPD, or other factors.might play more important role in prevent myopia shift.

In addition, poor compliance is an important problem for APL treatment. Further large sample and longer-period study is warranted.

CONCLUSIONS

Additional positive lenses during near work did not halt myopia shift in Chinese pre-myopic children during 6M follow-up.

Localizations of apolipoprotein A1 (ApoA1) in myopic and hyperopic chick retinas

Rachel K. M. Chun[1], C. L. Wong[1], K. K. Li[1], C. H. To[1,2]

[1]Laboratory of Experimental Optometry,
Centre for Myopia Research, School of Optometry,
The Hong Kong Polytechnic University, Hong Kong

[2]State Key Laboratory of Ophthalmology,
Zhongshan Ophthalmic Centre, Sun Yat-sen University,
GUANGZHOU, PR CHINA

Purpose

In our previous study, down regulation of retinal apolipoprotein A1 (ApoA1) was shown in both lens-induced and form deprivation myopic chicks using two-dimensional fluorescence difference electrophoresis (2D-DIGE). Moreover, increasing retinal ApoA1 level by intravitreal injection was able to inhibit myopia development. These findings suggested an important role of ApoA1 involved in ocular growth. We attempted to investigate the localization of retinal ApoA1 expression in myopic and hyperopic chicks.

Methods

Two-day-old white leghorn chicks (Gallus gallus domesticus) wore negative lenses (-10D) and positive (+10D) on their right and left eyes respectively for 3 days (n=4). Ocular dimensions were recorded using high frequency A-scan ultrasound system and the refractive errors were also measured by retinoscopy before and after lens wear. The chick eyes were then enucleated and fixed in 4% paraformaldehyde (PFA) and embedded in paraffin wax using Shandon Pathcentre Tissue Processor. The eye blocks were cut into 5μm thick sections by rotary microtome. Deparaffinization, rehydration and blocking (5% normal goat serum in PBS plus 0.3% Triton X-100) of sections were performed before probing against primary antibodies for ApoA1 (rabbit anti-chick ApoA1) and secondary antibodies (Alexa Fluor® 568 goat anti-rabbit IgG). The immunoreactivities of ApoA1 were then examined under with a fluorescence microscope (Nikon Eclipse Ti-S microscope).


Chick wearing -10D and +10D


Fixed eye and eye blocks


Rotary microtome

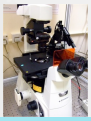
Fluorescence microscope

Results

The right eyes became myopic with a significant increase in the vitreous chamber depth (-2.75D±0.44, mean spherical equivalent ±SEM) after 3 days of -10D lens wear. The left eyes developed significant amount of hyperopia (+12.75D±0.24, mean±SEM) after wearing +10D lenses for 3 days (paired Student's t-tests, $p<0.05$). A decrease in vitreous chamber depth was also observed in hyperopic eyes (Fig.1). Immunoreactivities of ApoA1 were found in all layers in both myopic and hyperopic retinas. However, there were different distributions of ApoA1 between them. Stronger immunoreactivity of ApoA1 in myopic eye was found in outer segment of photoreceptor layer; whereas, the RPE and inner limiting membrane were more strongly labeled in the hyperopic retina (Fig.2).

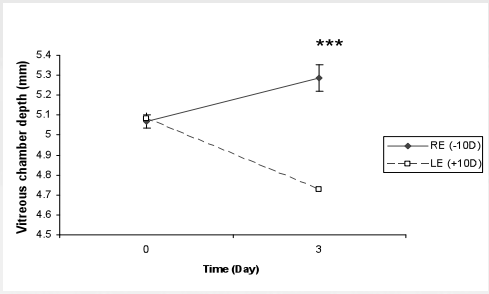

Fig.1 Vitreous chamber depth after 3 days of deprivation.
***p<0.001, paired t-test comparing right and left eyes

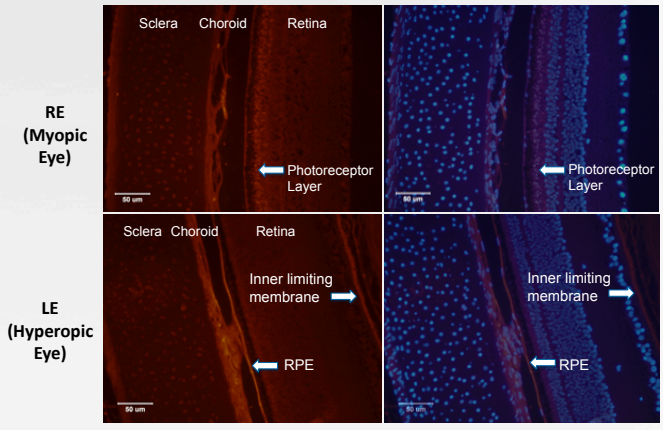

Fig.2. Localization of apolipoprotein A1 in myopic and hyperopic eye.

Discussion and conclusions

ApoA1 has been suggested as a "STOP" signal in the myopia development. This report showed different distributions of ApoA1 in myopic and hyperopic retinas for the first time. Since ApoA1 is the major component in high density lipoprotein which takes part in mediating lipid transport, the current results suggest there are changes of intraretinal lipid transport during different visual manipulations.

This work was supported by Myopia Niche Funding (J-BB7P), PolyU PhD studentship grant (RGL1) and PolyU research fund (G-YF97, B-Q15Q, G-U381),The Hong Kong Polytechnic University

Correspondence: sorachel@inet.polyu.edu.hk

Retinal *ANGPT2* and *UBE2N* expression after short term exposure to myopic and hyperopic defocus

41

Pamina Weber, Eva Burkhardt, Alexandra Marchã Penha, Marita Feldkaemper

Institute for Ophthalmic Research, Section of Neurobiology of the Eye, Tuebingen, Germany

INTRODUCTION

➢ Chick eyes compensate for the defocus imposed by positive or negative spectacle lenses[1]. From previous studies it is known that this involves retinal circuits[2,3].

➢ A previous microarray study (MA) focussed on gene expression changes in the amacrine cell layer (ACL) of chicks and found both, angiopoietin-2 (*ANGPT2*) and ubiquitin- conjugating enzyme E2N (*UBE2N*), to be differentially expressed[4].

➢ Both genes were therefore studied in more detail.

METHODS

➢ Chicks were either treated with +7 D or -7 D spectacle lenses or with no lenses for 4, 24, or 72 h (n=6 per group).

➢ Chicks were sacrificed and the fundal layers carefully dissected.

➢ Semi-quantitative real-time PCR (qPCR) was used for quantification of mRNA levels in the retina using β-actin and HPRT as reference genes.

➢ An additional group of animals (n=3) was treated with +7 D, -7 D, or no lens for 24 h and eyecups of these animals were used for in situ hybridization.

➢ DIG-labelled cRNA probes were prepared and hybridized to cryostat sections of the retinas.

RESULTS

Normalized expression in the whole retina

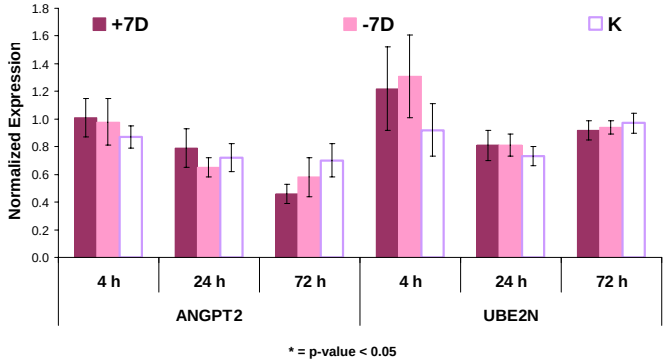

* = p-value < 0.05

Expression changes in the ACL and the whole retina after 24 h of treatment

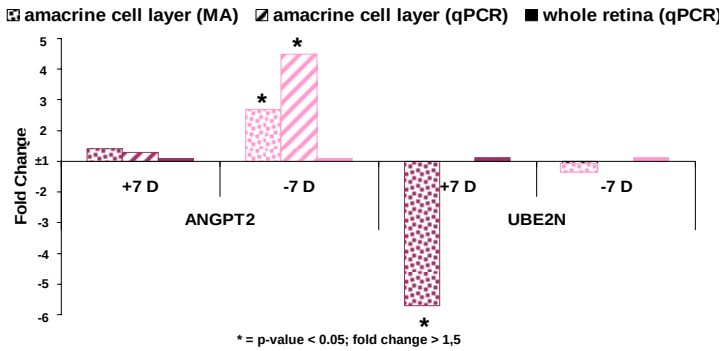

* = p-value < 0.05; fold change > 1,5

➢ *ANGPT2* and *UBE2N* expression did not change significantly in the whole retina samples after imposing negative or positive defocus for 4 hours, 24 hours or 3 days.

➢ The significant up-regulation of *ANGPT2* after minus lens treatment and down-regulation of *UBE2N* after plus lens treatment that was previously found in amacrine cell layer samples could therefore not be confirmed in the whole retina samples.

Localization of the mRNA in the retina

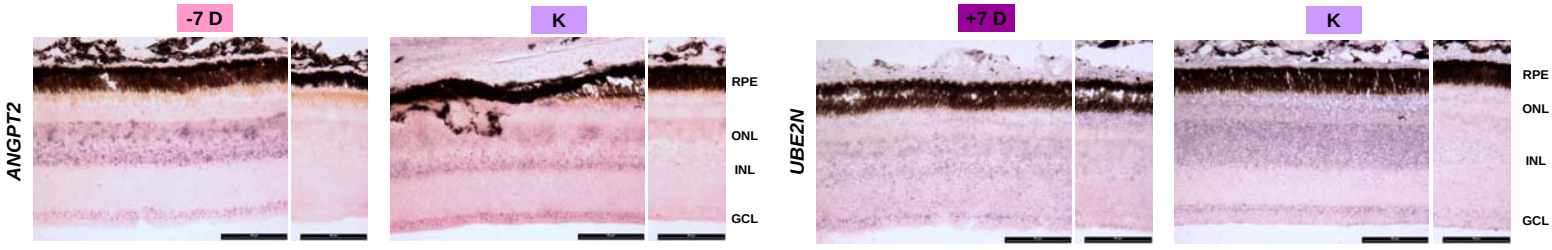

➢ Using in situ hybridization, mRNA for both genes were detected, especially in the inner nuclear layer (INL) and the ganglion cell layer (GCL)

➢ Focussing on the amacrine cell layer, the in situ hybridization results showed a similar trend in differential gene expression as with microarray and quantitative PCR (e.g. up-regulation of *ANGPT2* after 24 h of -7 D, down-regulation of *UBE2N* after 24 h of +7 D).

DISCUSSION

➢ Previous microarray results have shown a differential expression (fold change ≥ 1.5 with a p-value of ≤ 0.05) of both genes in the amacrine cell layer with a high up-regulation of *ANGPT2* following 24 h of minus lens treatment and a significant down-regulation of *UBE2N* after 24 h of +7 D treatment. The published differential expression of *ANGPT2* and *UBE2N* in the amacrine cell layer could no be validated by investigation of whole retina samples. This perhaps confirms the masking effect of the retina in case of changes in gene expression only in amacrine cells.

➢ In situ hybridization confirmed the expression of both genes in the INL. In addition, many cells in the ganglion cell layer express *ANGPT2* and *UBE2N.*

➢ We currently investigate, if a differential expression in response to defocus can be confirmed by using in situ hybridization methodology.

REFERENCES and ACKNOWLEDGMENT

This work was supported by the European Union Research Training Network "MyEuropia" MRTN-CT-2006-034021

[1] **Schaeffel F, Glasser A, Howland HC.** Accomodation, refractive error and eye growth in chickens. *Vision Res.* 1988;28(5):639-657

[2] **Wallman J.** Retinal control of eye growth and refraction. *Prog Retin Eye Res.* 1993;12:133-153

[3] **Stone RA.** Neural mechanisms and eye growth control. Tokoro T, ed. *Myopia Udates: proceedings of the 6th International Conference on Myopia.* Tokyo: Springer, 1997;241-254

[4] **Ashby AS, Feldkaemper M.** Microarray analysis of changes in gene expression within the amacrine cell layer of chicks following optical defocus. *Invest Ophthalmol Vis Sci.* 2010;51(7):3726-3735

Pupil diameter in emmetropia, myopia and hyperopia

Janis Orr, Lyle S. Gray, Dirk Seidel, Mhairi Day and Niall C. Strang
Department of Vision Sciences, Glasgow Caledonian University, Scotland

Purpose

•To investigate the relationship between target luminance, pupil diameter and accommodation in emmetropic, myopic and hyperopic subjects

Methods

•Thirty visually normal subjects (mean ± SD age: 25.36 ± 4.50 years) participated with informed consent in the experiment
•Refractive error (MSE) ranged from -5.00D to +4.00D; this was fully corrected using soft daily disposable contact lenses (1Day Acuvue J&J)
•Subjects with astigmatism >0.50DC were excluded
•Two target vergence levels presented at 0D and 3D
•Target luminance levels of 12, 99, 188, 388, 999, 1990 and 4111 cd/m^2 were presented in increasing order of luminance, using slides containing ND filters
•One minute of adaptation was allowed before readings were obtained at each luminance level
•Continuous recordings of monocular entrance (apparent) pupil diameter of 1 minute duration were obtained from the right eye using the Power Refractor II
•Ocular biometry measurements of corneal curvature and anterior chamber depth were taken using the IOLMaster(Zeiss) and actual pupil diameter was calculated

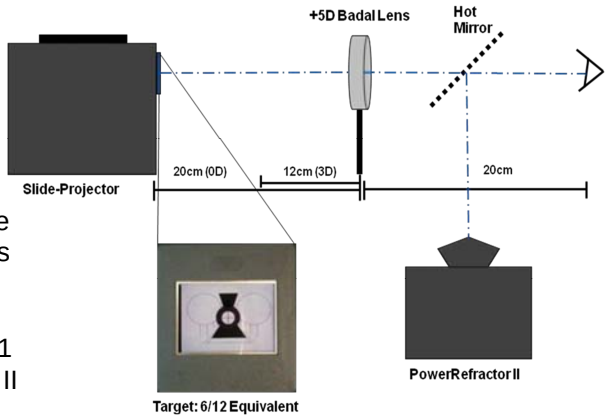

Results

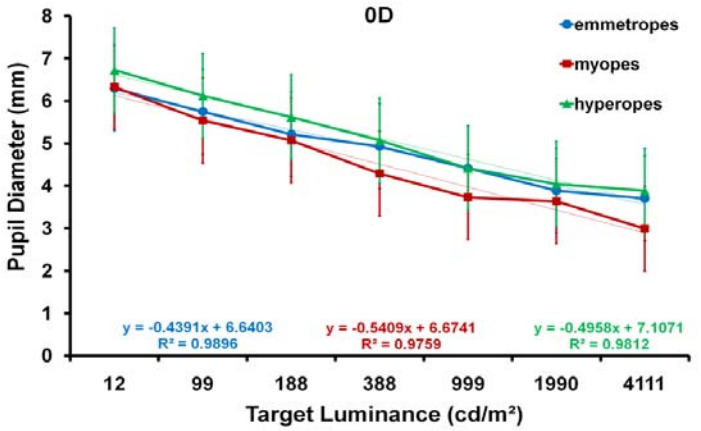

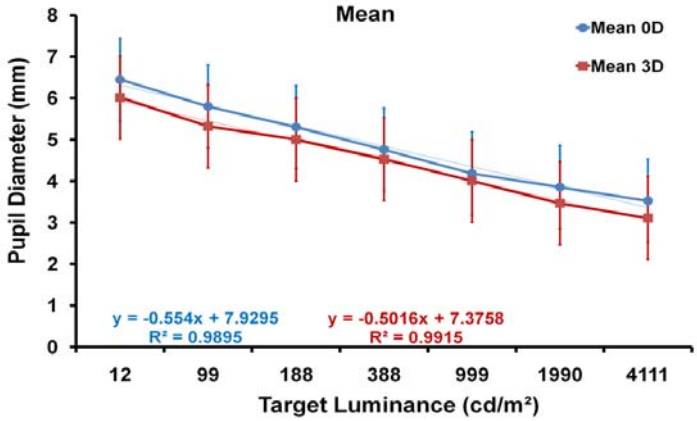

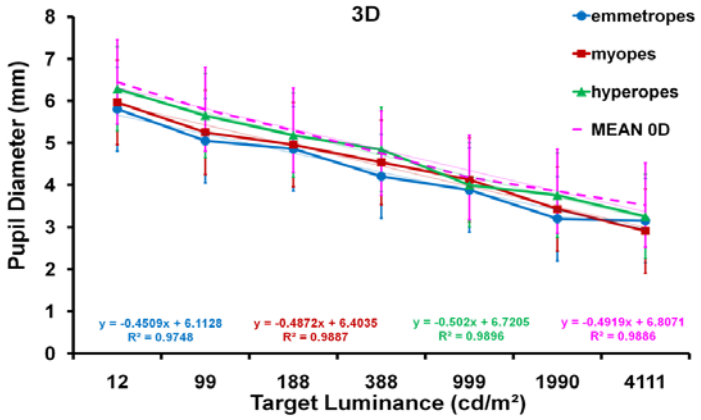

•Pupil diameter decreased significantly with increasing target luminance for all refractive groups at both accommodation stimulus levels (ANOVA, $p<0.005$ for all comparisons)
•Apparent and actual pupil diameters were not significantly different between the 0D and 3D accommodation stimulus levels for target luminances between 188-4111cd/m^2 but were significantly smaller at 3D for target luminances of 12cd/m^2 (ANOVA, $F_{1, 60}=3.348$, $p<0.05$) and 99cd/m^2 (ANOVA, $F_{1, 60}=3.429$, $p<0.05$)
•Pupil diameter was not significantly different between the refractive groups in any of the viewing conditions

Conclusions

1)Pupil diameter is determined by the interaction between the pupillary light response and near-induced miosis
2) At high luminance levels, near-induced miosis is overridden by the greater magnitude of the pupillary light response
3)Clinical measurements of apparent pupil diameter accurately relate to actual pupil diameter irrespective of refractive error

Accommodation in the deep-blue: *why do we over-accommodate and accept myopic defocus?*

Klaus Graef, Frank Schaeffel

Section of Neurobiology of the Eye, Ophthalmic Research Institute
Calwerstraße 7/1, 72076 Tübingen, Germany

Introduction

Longitudinal chromatic aberration (LCA) is a well known aberration of optical systems resulting from the fact that light of different wavelengths is focused at different distances. Light of shorter wavelengths is exposed to higher refractive indices than light of longer wavelengths. As a result, focal lengths are shorter in the blue than in the red. The LCA function is well established for the human eye (see figure 1, adapted by Marcos et. al. (1999)).

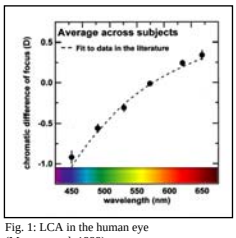

Fig. 1: LCA in the human eye (Marcos et. al. 1999)

One could expect that accommodation follows the function of the LCA. While this has been shown to be true between 700 to about 450 nm, a reversion occurs at even shorter wavelengths (see figure 2, adapted from Seidemann & Schaeffel, (2002)), which has been confirmed later by Rucker & Kruger, (2004).

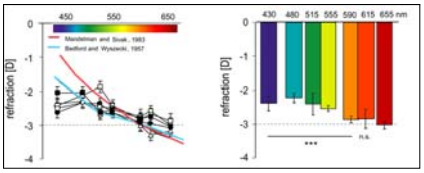

Fig. 2: Accommodation at different illumination conditions (Seidemann & Schaeffel, 2002)

Methods

Effects of LCA on accommodation were studied in emmetropes (n=5, 26.6 ± 1.5 years; mean SE -0.05 ± 0.1 D) and myopes (n=5, 27.4 ± 3.4 y; mean SE -1.9 ± 0.6). Refractive errors were corrected and all subjects had a visual acuity of logVA 0.0, or better. Accommodation was measured binocularly, using the PowerRefractor (Choi et al., 2000). The reading target (angular size of the letters 0.2°) was presented at a distance of 3D and illuminated either with white light or with quasi monochromatic light of 417, 431, 491 and 615 nm (experimental setup, see figure 3). Two-way paired t-tests were used to calculate significances. Three experiments were conducted:

Experiment (1): 4*5 cm reading target with continuous text, high luminance.
Experiment (2): 4*5 cm reading target with a single Landolt ring, high and low luminance.
Experiment (3): 1° (~6mm) reading target with a single Landolt ring, high luminance.

Fig. 3: Experimental setup

Results

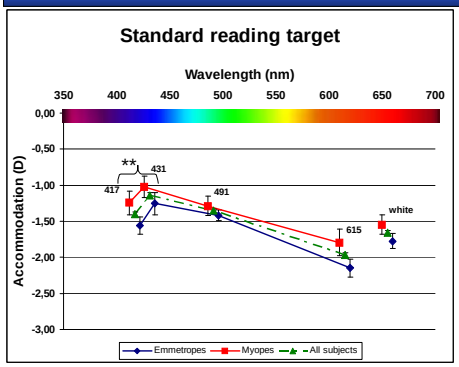

Fig. 5: Continuous text, 4*5 cm reading target

Experiment (1) Accommodation relaxed with decreasing wavelengths, as expected from LCA with the standard reading target. In line with the findings by Seidemann (2002), there was a significant increase in accommodation from 431 to 417 nm, ($p = 0.00145$). Figure 5 shows mean values ± SEMs. Values for myopes (-5nm) and emmetropes (5+nm) are shifted relative to each other for clarity.

Experiment (2) with high luminance. Confirmed the effects from experiment 1. With a defined, centered accommodation target, the significance level was even higher ($p < 0.001$) Figure 6 shows mean values ± SEMs. Values for myopes (-5nm) and emmetropes (5+nm) are shifted relative to each other for clarity.

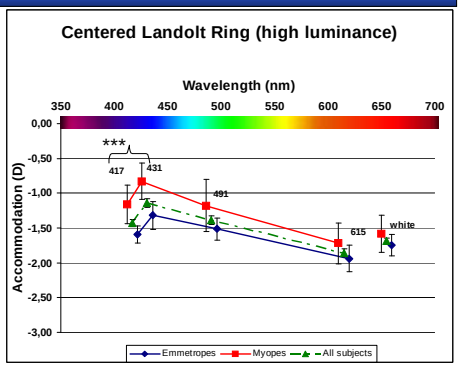

Fig. 6: Centered Landolt ring, 4*5 cm reading target

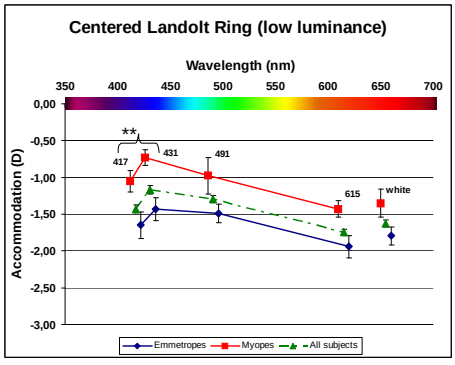

Fig. 7: Centered Landolt ring, 4*5 cm reading target,low luminance

Experiment (2) with low illuminance. This condition was set up to test the stability of this effect. Accommodation increased significantly from 431 to 417 nm ($p = 0.005$). Figure 7 shows mean values ± SEMs. Values for myopes (-5nm) and emmetropes (5+nm) are shifted for clarity.

Experiment (3) With a target that only stimulated the ("blue-free" fovea), the effect disappeared. Between 431 and 417nm, there was no significant increase in accommodation ($p = 0.582$, paired t-Test). Fig. 8 shows mean values ± SEMs. Values for myopes (-5nm) and emmetropes (5+nm) are shifted for clarity.

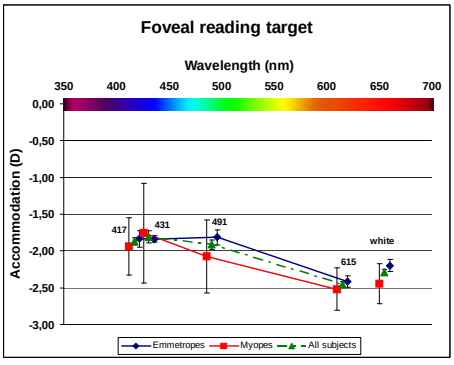

Fig. 8: Centered Landolt ring, 6mm diameter reading target

Conclusions

These results suggest that accommodation control through M and L cones is different from that of S-cones. It is possible that S-cones "prefer" the myopic defocus that they are exposed to under every day viewing conditions in polychromatic light. The fact, that over-accommodation is prohibited if the stimulation is only foveal (with little or no blue cones) supports the idea of an involvement of S-cones in overstimulation of accommodation.

References

Choi, M. et al. (2000). ***Optometry and Vision Science 77,*** **537-548**
Marcos S. et. al. (1999). ***Vision Research, 39,*** **4309-4323**
Rucker FJ & Kruger PB ***Vision Reseach 44,*** **197-208 (2004)**
Seidemann, A., & Schaeffel, F. (2002). ***Vision Research, 42,*** **2409–2417.**

Acknowledgement

This project has received funding from the Marie Curie Research Training Network "MyEuropia"

MRTN-CT-2006-034021

I would also like to thank Arne Ohlendorf, Tudor Tepelus and all subjects for their great support.

Peripheral objective blur thresholds in emmetropes and myopes

Lorraine A. Duffy, Mhairi Day, Dirk Seidel, Lyle S. Gray and Niall C. Strang
Department of Vision Sciences, Glasgow Caledonian University, Scotland

Aim

To measure objective blur thresholds as a function of target eccentricity in emmetropes (EMMs) and myopes (MYOs).

Methods

- 10 subjects: 5 EMMs 5 MYOs, MSE: -1.00DS to -7.00DS.
- MYOs fully corrected with daily disposable soft contact lenses.
- Targets composed of annulus (4cpd sine wave grating) on a uniform grey background **(Figure 1)**. Annulus was positioned to produce target eccentricities 0-8deg. Central fixation maintained with non accommodative red LED.

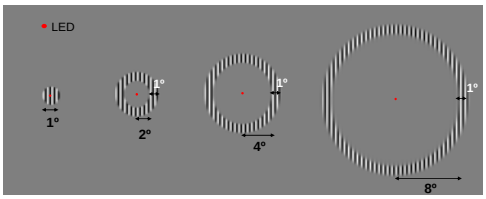

Figure 1: Four targets, radii altered to achieve four target eccentricities: central, 2, 4 and 8deg.

- Targets viewed monocularly with right eye, within a Badal (+5D) optical system. 2min continuous recording of accommodation response **(Figure 2)** and 10 static responses measured with modified, open field, infrared Shin-Nippon SRW-5000 autorefractor.
- Initial stationary response was recorded with subject viewing stationary central target positioned at pre-determined open-loop level **(Figure 2)**.
- Objective blur threshold **(OBT)** obtained, for each target eccentricity, by varying the oscillation amplitude sinusoidally (0.5Hz) around central point equal to subjects' open-loop level. Oscillation amplitude was varied randomly between 0.125 and 2.00D **(Figure 2)**.

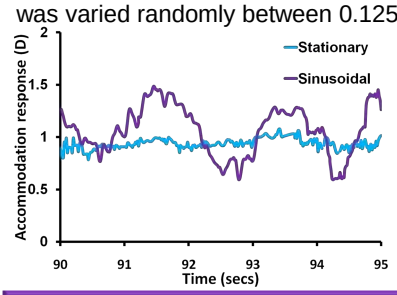

Figure 2: Continuous accommodation responses for stationary and sinusoidally moving target. Oscillation amplitude: 1.00D. Target eccentricity: central

- For each recording, 10 power spectra were obtained from FFT analysis averaged **(Figure 3)**.

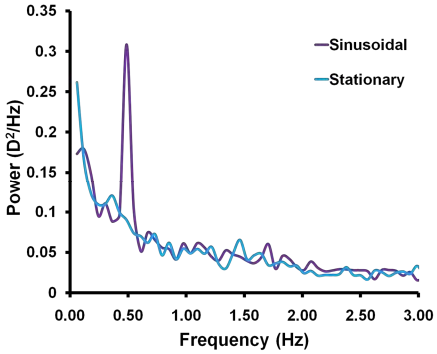

Figure 3: Mean power spectra for stationary and sinusoidally moving target. Oscillation amplitude: 1.00D. Target eccentricity: central.

- The total power and standard deviation (SD) calculated for 0.43-0.55Hz **(Figure 4)**. The total power for each oscillation amplitude was compared to the total power obtained for stationary target to determine the OBT for each target eccentricity **(Figure 4)**. The total power for each oscillation amplitude was compared to the total power obtained for stationary target (0Hz) to determine the OBT for each target eccentricity **(Figure 4)**.

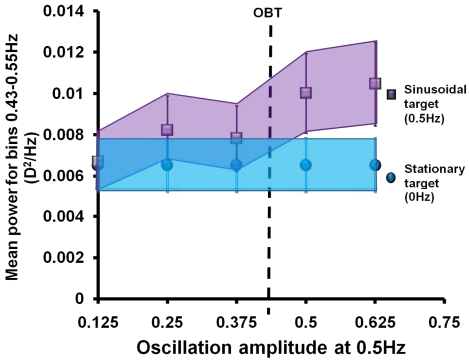

Figure 4: Mean power SD for each oscillation amplitude for sinusoidal target compared to stationary target. OBT: (0.375+0.5)/2 = 0.4375D

Results

- To show no change in the mean accommodation response throughout the experiment mean SD of 10 static responses was plotted **(Figure 5)**.
- No significant effect of eccentricity (ANOVA, $F_{3,16}$=1.511, p=0.219)
- No significant difference between refractive groups (ANOVA, $F_{1,13}$=0.89, p=0.36)
- No significant effect of oscillation amplitude (ANOVA, $F_{8,38}$=1.138, p=0.367)

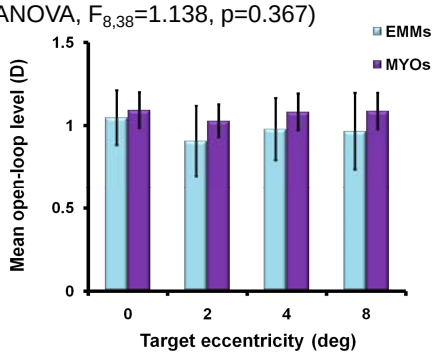

Figure 5: Mean accommodation response (D), with eccentricity, for EMMs and MYOs. Error bars are s.e.m.

- Objective blur thresholds increased linearly with eccentricity in both EMMs (ANOVA, $F_{3,16}$=12.66, p<0.05) and MYOs (ANOVA, $F_{3,16}$=42.88, p<0.005) **(Figure 6)**
- Significant difference in gradient of linear regression between EMMs and MYOs (t-test, t_9=3.20, p<0.05)
- No significant difference in objective blur thresholds between refractive groups at 0deg (ANOVA, p=0.342) and 2deg (ANOVA, p=0.301).
- MYOs had significantly larger blur thresholds than EMMs at 4deg (ANOVA, p<0.05) and 8deg (ANOVA, p<0.001).

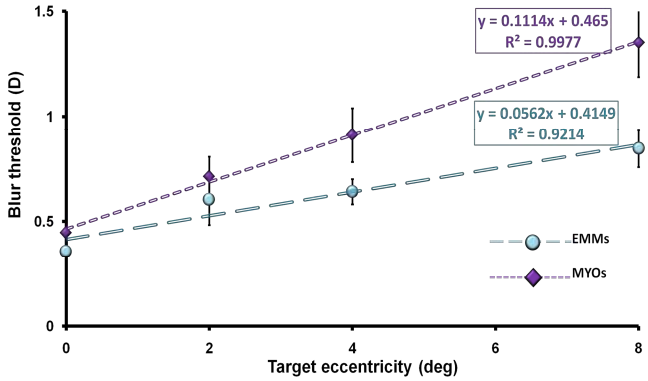

Figure 6: Mean blur thresholds with eccentricity for EMMs and MYOs. Error bars are s.e.m.

Discussion and Conclusions

- Objective blur thresholds increase systematically with target eccentricity in all subjects
- The rate of increase in objective blur thresholds with eccentricity is twice as large in MYOs than EMMs
- Larger blur thresholds in MYOs may exaggerate the effect of peripheral hyperopic defocus found in MYOs

Corresponding Address: lorraine.duffy@gcu.ac.uk

Spatial visual performance with simulated and real spherical and astigmatic defocus

Arne Ohlendorf[1]*, Juan Tabernero[2] and Frank Schaeffel[1]

[1]Institute for Ophthalmic Research, Section of Neurobiology of the Eye, Tuebingen, Germany

[2]Laboratorio de Optica, Universidad de Murcia, Spain

Introduction

Astigmatism is the second major refractive distortion. It is known to be largely genetically determined and mostly corneal. The corneal origin can partially be explained by the mechanical pressure of the eye lid in the vertical pupil meridian. Astigmatism shows a typical age-dependent prevalence - high at very young age, less in the middle age and a later increase at pre-presbyopic age.
In our experiments, we compared the effect of simulated and real spherical and astigmatic defocus on visual acuity (VA).

Methods

Effects of simulated (SIM) and lens-induced (OPT) spherical and astigmatic defocus on visual acuity was studied in 5 subjects (3 emmetropes (-0.16 ± 0.14 D) and two myopes (M1 -2.00 D, M2 -1.00 D). Mean age was 27 ± 2.3 years and all subjects had a VA of logVA = 0.1. Defocus was simulated with the Liou-Brennan eye model using ZEMAX, and real defocus was induced with trial lenses. All subjects had an artificial pupil with a diameter of 3 mm. Three different experiments were conducted in which visual acuity was reduced by 20% (logVA 0.0), 50% (logVA -0.2) and 75% (logVA -0.5) by the following three methods: (1) imposing positive spherical defocus, (2) imposing positive and negative astigmatic defocus in three axes (0°, 45° and 90°) and (3) imposing a spherical equivalent of 0 D with positive and negative astigmatic lenses in the same three axes as in (2).

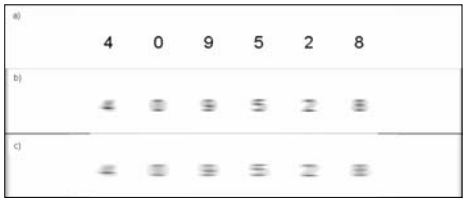

Figure 1. Examples of the simulations of astigmatic defocus using ZEMAX and the Liou-Brennan eye model. (A) acuity chart of logVA -0.2 for a test distance of 4 m with no defocus, (B) with astigmatic defocus of +0.75 D at 90° and (C) with astigmatic defocus of +1.00 D at 90°

Results

Experiment 1: Real and simulated spherical defocus.
There was no significant difference in visual acuity with simulated and lens-induced positive spherical defocus (difference between simulated and real defocus for logVA 0.0: p=0.07, logVA -0.2: p=0.051, logVA -0.5: p=0.09)

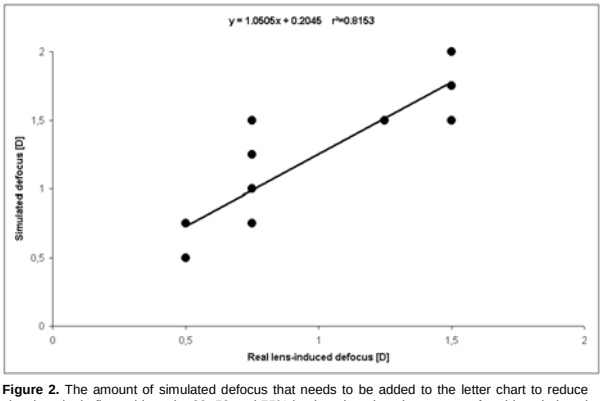

Figure 2. The amount of simulated defocus that needs to be added to the letter chart to reduce visual acuity in five subjects by 20, 50 and 75% is plotted against the amount of real lens-induced defocus that is necessary to achieve the same reduction.

Experiment 2: Real and simulated astigmatic defocus
There were no differences in readability when targets were presented with astigmatism simulated at different axes; also the sign of astigmatic defocus had little effect (there were minor differences due to the spherical aberrations of the eye model). However, there were striking differences in visual acuity when atsigmatsim was simulated or real. For all tested acuities, the difference between SIM and OPT was significant (p<0.001).

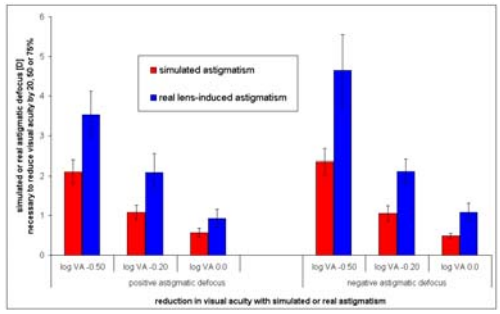

Figure 3. Astigmatic defocus to reduce visual acuity by 75, 50 or 20% Mean absolute values ± standard deviations.

Experiment 3: Real and simulated cross-cylinder defocus
There were no differences in visual acuity when the simulated or real astigmatic defocus was imposed in the three axes. However, there were, again, striking differences in the tested visual acuity for SIM and OPT (p<0.001).

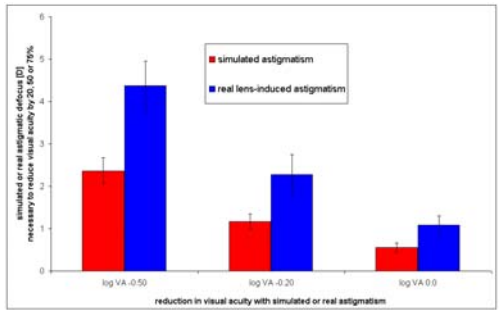

Figure 4. Cross-cylinders defocus to reduce visual acuity by 75, 50 and 20% Mean absolute value ± standard deviation

Conclusion

The effect of spherical defocus on visual acuity can be nicely predicted by simulation - but the visual system appears to be more tolerant against real astigmatic defocus, compared to simulated astigmatic defocus. Possible explanations are (1) higher ocular aberrations could help to improve visual acuity in the presence of astigmatism, (2) fluctuations of accommodation could permit to extract more details from the letter chart in the presence of astigmatic defocus.
However, both explanations are weak because the amount of imposed astigmatisc defocus was much higher than the equivalent defocus from human higher-order aberrations (0.3 D versus 1-4 D of imposed defocus), and also the far accommodation (around 0.25 D) available to the subjects was much less than the imposed defocus.
Therefore, something appears special about the visual processing of real astigmatic defocus - it appears to have less effect on visual acuity than simulations predict.

Acknowledgment:
This study was supported by the Centre for Integrative Neuroscience (CIN) Tuebingen.

*contact: arne.ohlendorf@klinikum.uni-tuebingen.de

This work was supported by the College of Optometrists Research Fellowship Award

A head-mounted, open-field, binocular device to measure and analyse pupil size and refractive error in real-time

Mhairi Day, Dirk Seidel, Niall C. Strang and Lyle S. Gray
Department of Vision Sciences, Glasgow Caledonian University, Scotland
m.day@gcu.ac.uk

Aim

To develop a portable, accurate, head-mounted device that measures pupil size & refractive error in a natural environment.

Methods

Instrumentation

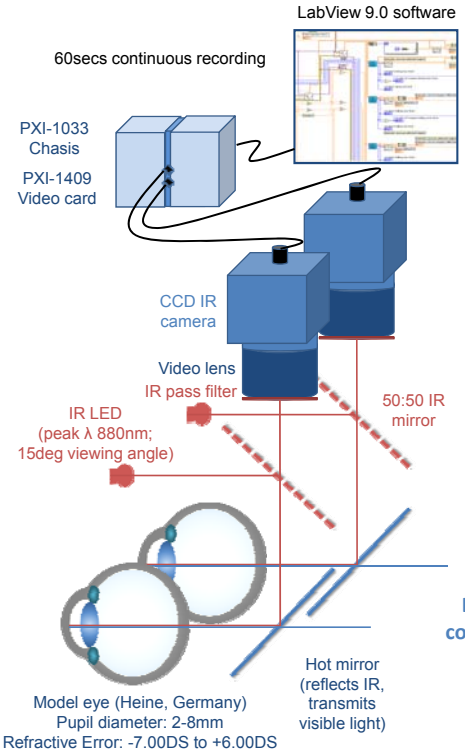

Analysis

Pupil diameter

- Pupil edges detected using edge detection:
  - radial lines across the pupil 0.25degrees apart
  - edge (●) = 90% contrast over 2 neighbouring pixels
- Best fit circle plotted (◯) & diameter measured

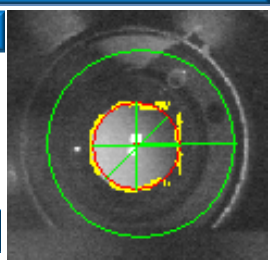

Refractive error

- Measured for a pupil diameter of 5mm
- Intensity along vertical, horizontal & oblique (45deg) meridians plotted
- Luminance gradient = Δ intensity / number of pixels

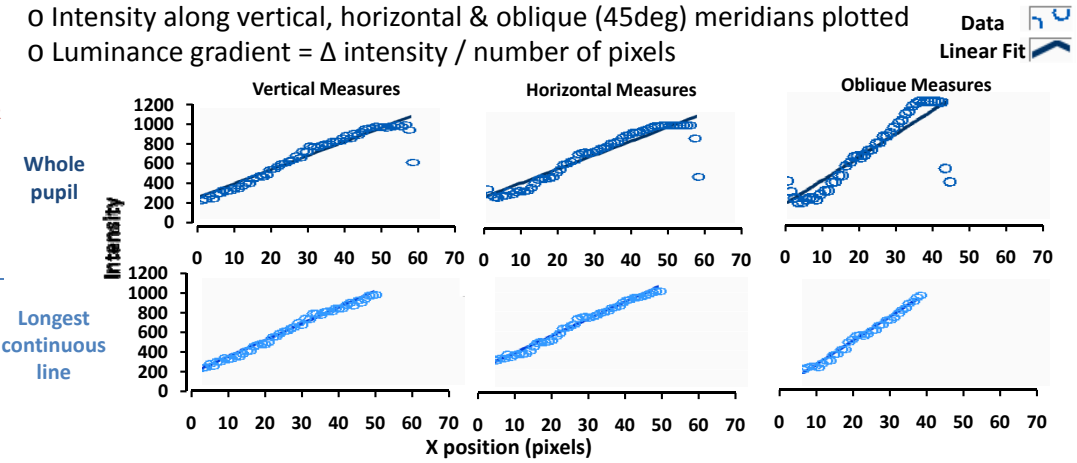

Results

Pupil diameter

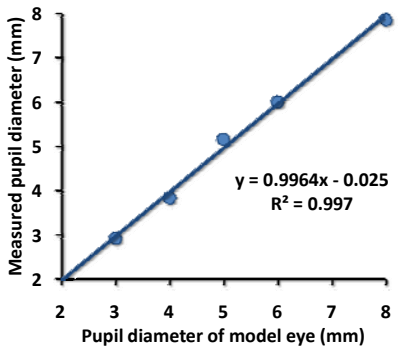

Refractive Error

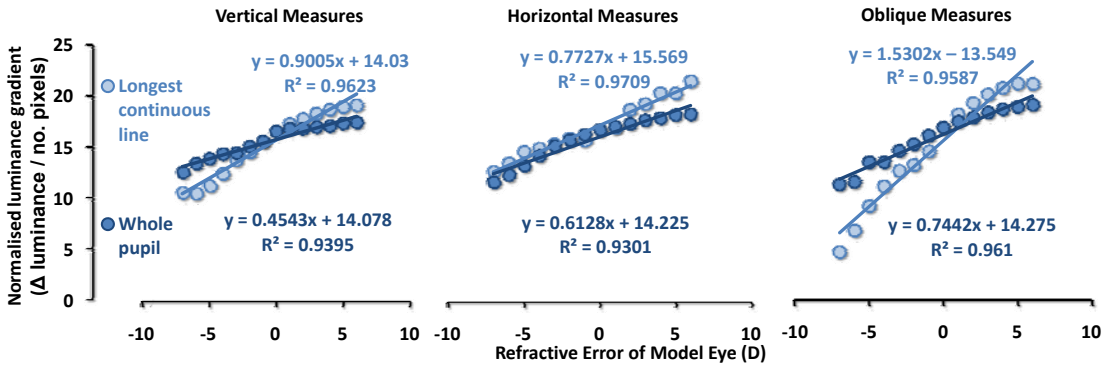

Discussion & Conclusions

High resolution measurements of pupil diameter & refractive error can be made & analysed simultaneously from two eyes in a system allowing binocular, open-field viewing.

More accurate measurements of refractive error can be made by selecting the longest continuous line of luminance gradient within the pupil, eliminating effects near the pupil edge & from the bright corneal reflex.

Accurate measurements along multiple meridians allows future developments in programming to calculate astigmatism & peripheral refraction along with measurements of eye position using the corneal reflex.

This will ultimately provide a comprehensive description of the ocular motor system allowing comparison between refractive groups in naturalistic conditions that may provide insight into the current understanding of myopia.

Development of optical techniques for myopia research

Frank Schaeffel[1], Hakan Kaymak[2], Juan Tabernero[1,3]

[1]Section of Neurobiology of the Eye, Calwerstrasse 7/1, 72076 Tübingen, Germany; [2]Breyer-Augenchirurgie, 40212 Düsseldorf, Germany; [3]Laboratorio de Optica, Universidad Murcia, 30071 Murcia, Spain
e-mail: frank.schaeffel@uni-tuebingen.de
http://www.uak.medizin.uni-tuebingen.de/frank/

all devices are available through the Steinbeis Centre for Biomedical Optics and Functional Testing, Tübingen (Director: Prof. E. Zrenner) http://www.stz-biomed.de/

Eccentric Infrared Photorefraction in animal models

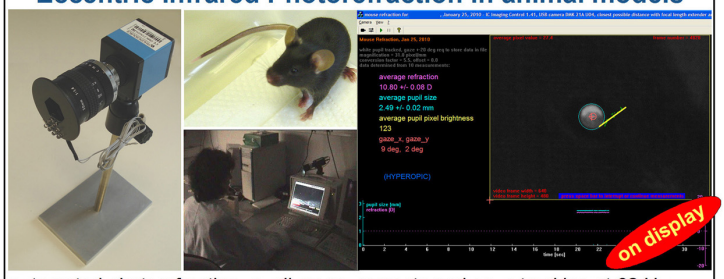

automated photorefraction, pupil measurements and gaze tracking at 62 Hz (USB2 cameras - all electric power comes from the USB port of the laptop)

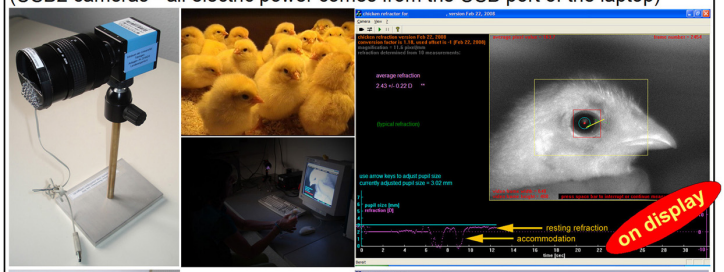

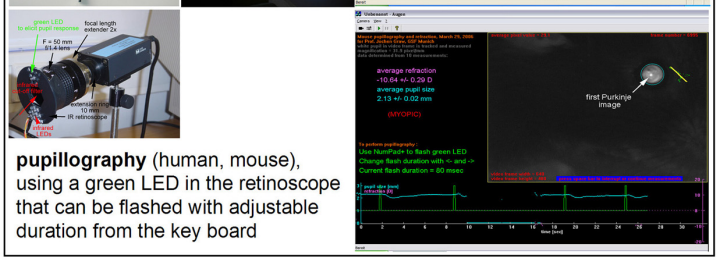

pupillography (human, mouse), using a green LED in the retinoscope that can be flashed with adjustable duration from the key board

Eccentric Infrared Photorefraction in humans

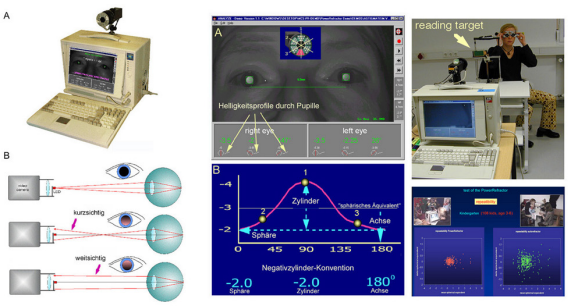

automated binocular refraction, pupillography and vergence measurements from 1 m distance at 50 Hz (PAL format)

*available through Plusoptix http://www.plusoptix.de - **see their booth at this meeting***
(no current involvement of the authors)

Automated Photokeratometry

corneal radius of curvature is measured by detection of the Purkinje images of eight infrared LEDs, arranged in a circle, and fitting their positions with a circle at 62 Hz frame rate. The techniques runs from a labtop and works in alert animals (chick, mouse, chameleon, etc).

Calibration occurs with a single ball bearing of known radius of curvature.

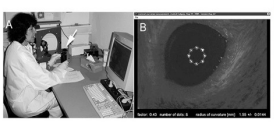

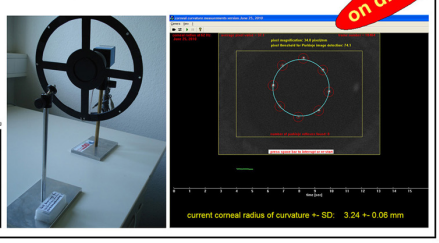

Scanning Infrared Photorefractor

continuous refraction in the vertical pupil meridian over the central 90 deg of the visual field in 3 seconds (180 measurements) - second scan in the horizontal pupil meridian

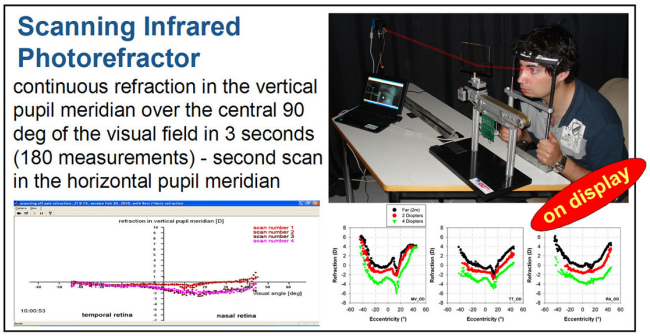

High spatial resolution video gaze tracking

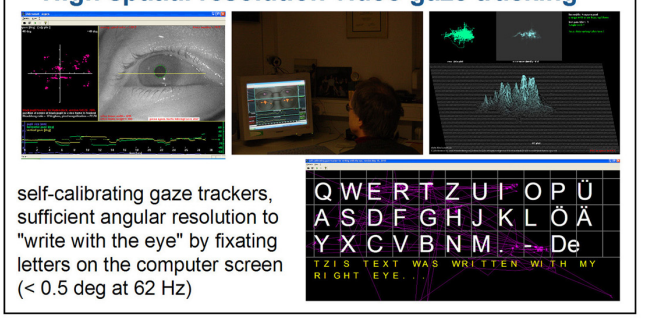

self-calibrating gaze trackers, sufficient angular resolution to "write with the eye" by fixating letters on the computer screen (< 0.5 deg at 62 Hz)

Automated quantification of optomotor responses

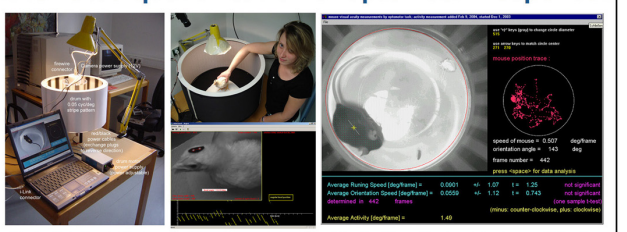

whole body optomotor responses of mice in the drum are quantified. Chicken head nystagmus is tracked after attaching a black card board with two white dots to the feathers on the top of the head.

Measurement of crystalline lens tilt and decentration

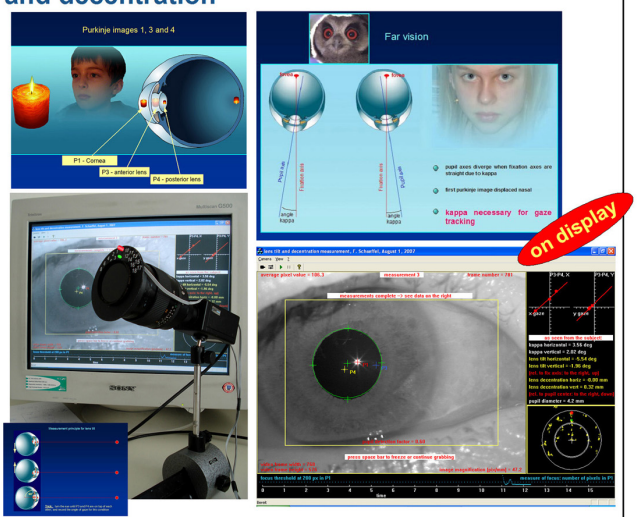

non-invasive, automated and fast technique to measure the decentration and tilt of the the natural and artificial lens in the eye